

# SGR A\* POLARIZATION: NO ADAF, LOW ACCRETION RATE, AND NON-THERMAL SYNCHROTRON EMISSION

ERIC AGOL

Physics and Astronomy Department, Johns Hopkins University, Baltimore, MD 21218; agol@pha.jhu.edu

*Draft version April 3, 2019*

## ABSTRACT

The recent detection of polarized radiation from Sgr A\* requires a non-thermal electron distribution for the emitting plasma. The Faraday rotation measure must be small, placing strong limits on the density and magnetic field strength. We show that these constraints rule out advection-dominated accretion flow models. We construct a simple two-component model which can reproduce both the radio to mm spectrum and the polarization. This model predicts that the polarization should rise to nearly 100% at shorter wavelengths. The first component, possibly a black-hole powered jet, is compact, low density, and self-absorbed near 1 mm with ordered magnetic field, relativistic Alfvén speed, and a non-thermal electron distribution. The second component is poorly constrained, but may be a convection-dominated accretion flow with  $\dot{M} \sim 10^{-9} M_{\odot}/\text{yr}$ , in which feedback from accretion onto the black hole suppresses the accretion rate at large radii. The black hole shadow should be detectable with sub-mm VLBI.

*Subject headings:* accretion, accretion disks — black hole physics — polarization — Galaxy: center

## 1. INTRODUCTION

The nearest supermassive black hole candidate lies at the center of the Milky Way galaxy, weighing in at  $2.6 \times 10^6 M_{\odot}$ , as inferred from motions of stars near the galactic center (Ghez et al. 1998; Genzel et al. 1997). The low luminosity of the point source associated with the center,  $\lesssim 10^{37}$  erg/s, is a conundrum since accretion from stellar winds of neighboring stars should create a luminosity of  $\sim 10^{41}$  erg/s. One possibility is that most of the energy is carried by the accreting matter into the black hole, as in the advection-dominated accretion flow solution (ADAF, Narayan & Yi 1994; Narayan, Yi, & Mahadevan 1995). Such a situation is achieved when most of the dissipated energy is channeled into protons which cannot radiate efficiently. Low efficiency also occurs when gas accretes spherically and carries its energy in as kinetic energy (Melia 1992). Alternatively, the accretion rate may be overestimated, and the emission may be due to a tenuous disk or jet.

The radio spectrum of Sgr A\* can be described by a power law,  $F_{\nu} \propto \nu^{1/3}$  from centimeter to millimeter wavelengths. This is intriguingly close to the spectrum of optically thin, mono-energetic electrons emitting synchrotron radiation (Beckert & Duschl 1997). However, this explanation is not unique: a self-absorbed source which varies in size as a function of frequency may produce a similar spectral slope (Melia 1992; Narayan et al. 1995). A possible technique to distinguish these models is to measure the polarization of the emission: Faraday rotation and self-absorption can change the polarization magnitude and wavelength dependence (Jones & O'Dell 1977).

Only recently has linear polarization been detected (Aitken et al. 2000: A00); previous searches showed only marginal detections or upper limits (Bower et al. 1999a,b). After correcting for contamination by dust and free-free emission, the inferred polarization is 10-20%, implying a synchrotron origin. Remarkably, the polarization shows a change in position angle of  $\sim 90^{\circ}$  around 1 mm, which

A00 suggest might be due to synchrotron self-absorption. We first discuss the physics of synchrotron polarization (§2); we then apply it to various models in the literature (§3); next we discuss a model consistent with all of the observations (§4); and finally speculate on the physical implications of this model (§5).

## 2. SYNCHROTRON THEORY BACKGROUND

In the synchrotron limit ( $\gamma \gg 1$ ) for an isotropic electron velocity distribution, some analytic results have been derived, which we now summarize (Ginzburg & Syrovatskii 1965 & 1969: GS). For a uniform slab of electrons with a power-law distribution,  $dn_e/d\gamma \propto \gamma^{-\xi}$  (with  $\gamma_{min} \leq \gamma \ll \gamma_{max}$  such that electrons with  $\gamma_{min}$  and  $\gamma_{max}$  do not contribute to the frequency of interest), we can relate the magnetic field strength and electron density in the slab to the fluid-frame brightness temperature and the spectral turnover due to self-absorption. For  $\xi = 2$  and a uniform field  $B_{\perp}$  (projected into the sky plane) we find  $B_{\perp} \sim 2T_{11}^{-2}\nu_{12}$  G and  $\tau_C \sim 3 \times 10^{-2}T_{11}^4\nu_{12}\gamma_{min}^{-1}$ , where  $T_{11}$  is the brightness temperature in units of  $10^{11}$  K at the self-absorption frequency  $\nu_t = 10^{12}\nu_{12}$  Hz and  $\tau_C$  is the Compton scattering optical depth of the emission region. For  $\nu < \nu_t$ , the emission is self-absorbed so  $F_{\nu} \propto \nu^{5/2}$ , while above this frequency the emission is optically-thin and  $F_{\nu} \propto \nu^{(1-\xi)/2} \exp(-\nu/\nu_{max})$  where  $\nu_{max} = 3B_{\perp}e\gamma_{max}^2/(4\pi m_e c)$ .

In the optically-thin regime, the polarization plane is perpendicular to the magnetic field with polarization  $\Pi = (\xi + 1)/(\xi + 7/3)$ , up to 100% for  $\xi \gg 1$ . In the optically-thick regime,  $\Pi = -3/(6\xi + 13)$  (for  $\xi > 1/3$ ); the radiation polarized perpendicular to the magnetic field is absorbed more strongly than the opposite polarization, causing the radiation polarized along the magnetic field to dominate, switching the polarization angle by  $90^{\circ}$ , which changes the sign of  $\Pi$ . Numerical calculations show that the optically-thick polarization peaks at  $|\Pi| = 20\%$  for  $\xi = 1/3$ , but remains large for  $0 < \xi < 2$ .

To compute the polarization near the self-absorption frequency requires a knowledge of the polarized opacity and emissivity,  $\mu_{\perp,\parallel}, \epsilon_{\perp,\parallel}$ . For  $\xi = 2$ , these can be approximated as (GS):  $\mu_{\perp,\parallel} = r_s^{-1}(\nu/\nu_t)^{-3}(1 \pm 3/4)$  and  $(\epsilon_{\perp,\parallel}/\mu_{\perp,\parallel}) = 2S_t/9(\nu/\nu_t)^{5/2}(13 \pm 9)/(4 \pm 1)$  where  $r_s$  is the size of the emission region,  $\nu_t$  is the frequency for which the total source has an optical depth of unity (i.e.  $\tau = \mu r_s = 1/2(\mu_{\perp} + \mu_{\parallel})r_s = 1$ ),  $S_t$  is the source function near the frequency  $\nu_t$ , and the + or - signs go with the radiation emitted  $\perp$  or  $\parallel$  to the magnetic field, respectively. GS then express the polarization and emission for a slab with uniform magnetic field strength and direction, constant density, and size  $r_s$ :  $I_{\perp} = (\epsilon_{\perp}/\mu_{\perp})(1 - \exp(-\mu_{\perp}r_s))$ ,  $I_{\parallel} = (\epsilon_{\parallel}/\mu_{\parallel})(1 - \exp(-\mu_{\parallel}r_s))$ , and  $\Pi = (I_{\perp} - I_{\parallel})/(I_{\perp} + I_{\parallel})$ , where  $I_{\perp}, I_{\parallel}$  are the intensities (erg/cm<sup>2</sup>/s/Hz/sr) with polarization perpendicular and parallel to the projected direction of the magnetic field on the sky.

For electron distributions which are highly peaked at a single energy (such as mono-energetic or relativistic Maxwellian) the polarization for  $\nu \lesssim \nu_t$  is zero.

The Faraday effect rotates the polarization vector of photons emerging from different optical depths by different amounts, causing a cancellation in polarization (Agol & Blaes 1996). The differential Faraday rotation angle within the source scales as  $\Delta\theta = 3.6 \times 10^{28} \tau_{\text{phot}} B \nu^{-2} \gamma_{\text{min}}^{-2}$  (Jones & O'Dell 1977), where  $\tau_{\text{phot}}$  is the optical depth of the photosphere. When optically thin,  $\tau_{\text{phot}} \sim \tau_C$  is constant, so rotation is largest at the self-absorbed wavelength. When self-absorbed,  $\tau_{\text{phot}}$  of the photosphere scales as  $\nu^{\xi/2+2}$ , so the differential Faraday rotation angle  $\propto \nu^{\xi/2}$  (for  $\xi > 1/3$ ), again largest at the self-absorption wavelength. The differential rotation at  $\nu_t$  is  $\Delta\theta \sim 2\pi g(\xi)(\theta_b/\gamma_{\text{min}})^{\xi}/\gamma_{\text{min}}$ , where  $\gamma_{\text{min}}$  is the minimum electron Doppler factor,  $g(\xi)$  is a dimensionless factor of order unity, and  $\theta_b$  is the brightness temperature in units of  $m_e c^2/k_B$ .

### 3. OBSERVATIONAL CONSTRAINTS ON PUBLISHED MODELS

The observations of polarization in Sgr A\* provide the following constraints on emission models:

- 1) The Faraday rotation angle near the self-absorbed wavelength must be  $\ll \pi$ .
- 2) The electron distribution must be non-thermal since thermal emission is unpolarized when self-absorbed. If the beam correction by A00 is correct, then  $\Pi \sim 12\%$  at self-absorbed wavelengths, requiring  $\xi \lesssim 2$ .
- 3) The self-absorption frequency must lie near the change in polarization angle,  $\sim 1\text{mm}$ .
- 4) The component contributing at lower frequencies must have zero linear polarization.
- 5) The magnetic field must be ordered to prevent cancellation of polarization.

These constraints rule out nearly several models proposed in the literature, as will be discussed in turn.

The low efficiency of an ADAF implies a higher accretion rate and thus higher density than for a high efficiency flow of the same luminosity and geometrical thickness. For Sgr A\*, an accretion rate of  $\sim 10^{-(4-5)} M_{\odot}/\text{yr}$  is inferred due to capture of gas in the vicinity of the black hole

<sup>1</sup>Mahadevan (1999) and Özel, Psaltis, & Narayan (2000) have added a non-thermal electron component to ADAF models which contributes to the flux at wavelengths longer than 2 mm, not at the polarized wavelengths.

(Quataert, Narayan, & Reid 1999; Coker & Melia 1999), which is the value assumed in ADAF models. Assuming that the gas falls in at near the free-fall speed, one infers an electron density  $n_e = 10^{10} \text{ cm}^{-3} \dot{m}_{-5} x^{-3/2}$  and a magnetic field strength of  $B = 10^3 G \dot{m}_{-5}^{1/2} x^{-5/4} (v_A/0.1 v_{\text{ff}})$ , where  $x$  is the radius of the emission region in units of  $r_g = GM/c^2$ ,  $\dot{m}_{-5}$  is the accretion rate in units of  $10^{-5} M_{\odot}/\text{yr}$ , and  $v_A/v_{\text{ff}}$  is the ratio of the Alfvén speed to the free-fall speed. These values imply a total Faraday rotation angle at the self-absorption frequency  $\nu_t$  of  $\Delta\theta \sim 10^4 \dot{m}_{-5}^{3/2} \nu_{12}^{-2} (v_A/0.1 v_{\text{ff}})$ . This value is so large that rotation of the emitted radiation leads to zero net polarization, so ADAFs are in direct conflict with the observed polarization. Only significant modifications of the model, such as a reduction in the accretion rate by a factor of  $10^{-3}$ , can reduce the Faraday rotation angle  $\ll \pi$ . An accretion rate of  $10^{-8} M_{\odot}/\text{yr}$  is consistent with the observed luminosity if the accretion flow has a higher efficiency  $\sim 2\%$ , no longer “advection-dominated.” In addition, ADAF models assume a Maxwellian electron distribution, which cannot produce the observed switch in polarization angle<sup>1</sup>. Finally, ADAFs predict a higher self-absorption frequency: Özel et al. (2000) find that  $\nu_t \sim 5 \times 10^{12} \dot{m}_{-5}^{5/9} \text{ Hz}$ , which implies  $\dot{M} \sim 4 \times 10^{-7} M_{\odot}/\text{yr}$  to be consistent with the observed  $\nu_t \sim 5 \times 10^{11} \text{ Hz}$ . The accretion rate might be reduced if there is significant gas lost by a wind or jet (Begelman & Blandford 1999; Quataert & Narayan 1999) or if the Bondi rate is reduced by heating the infalling gas with heat carried outwards by a convection-dominated accretion flow, or “CDAF” (Stone, Pringle, & Begelman 1999; Quataert & Gruzinov 2000).

The model of Melia (1992) is rather similar to the ADAF model, and thus suffers the same problems: the high accretion rate implies high density which is inconsistent with the observed polarization.

Beckert & Duschl (1997) considered several 1-zone, quasi-monoenergetic and thermal emission models for the synchrotron emission. As we have pointed out, these electron distributions produce zero polarization when self-absorbed, and so are ruled out. Falcke, Mannheim, & Biermann (1993) present a disk-plus-jet model which assumes a tangled magnetic field topology which would erase any polarization. The model is not described in enough detail to easily ascertain whether it predicts the correct self-absorption frequency or small Faraday rotation.

### 4. A PHENOMENOLOGICAL MODEL

Now, we attempt to construct a model consistent with all of the data, using uniform emission regions for simplicity. Typical optically-thin AGN spectra show  $\xi \sim 2 - 3$ ; since  $\xi = 2$  is consistent with the polarization from A00, we fix  $\xi = 2$  in our model fits. The model parameters for the polarized component are  $S_t = 6 \text{ Jy}$ ,  $\nu_t = 550 \Gamma^{-1} \text{ GHz}$  (corresponding to  $\lambda = 0.55 \text{ mm}$ ), and  $\nu_{\text{max}} \sim 5000 \Gamma^{-1} \text{ GHz}$ , where  $\Gamma$  is the bulk Doppler boost parameter (Figure 1).

To explain the lack of polarization and spectral slope flatter than  $5/2$ , we require an additional component which is unpolarized and has a cutoff near 1 mm so that it doesn't dilute the polarization at shorter wavelengths. Since Sgr

A\* has a spectral slope of  $1/3$  at mm wavelengths and appears to have a spectral turnover at  $1$  GHz, we model the spectrum as a monoenergetic electron distribution with energy  $\gamma$  and zero polarization (due to Faraday depolarization or tangled magnetic field) which becomes self-absorbed at low frequency. For the unpolarized component, we find  $F_\nu = 1.3(\nu/\nu_{max})^{1/3} \exp(-\nu/\nu_{max})$  Jy with  $\nu_{max} \sim 50$  GHz, and  $\nu_t \sim 1$  GHz (Figure 1).

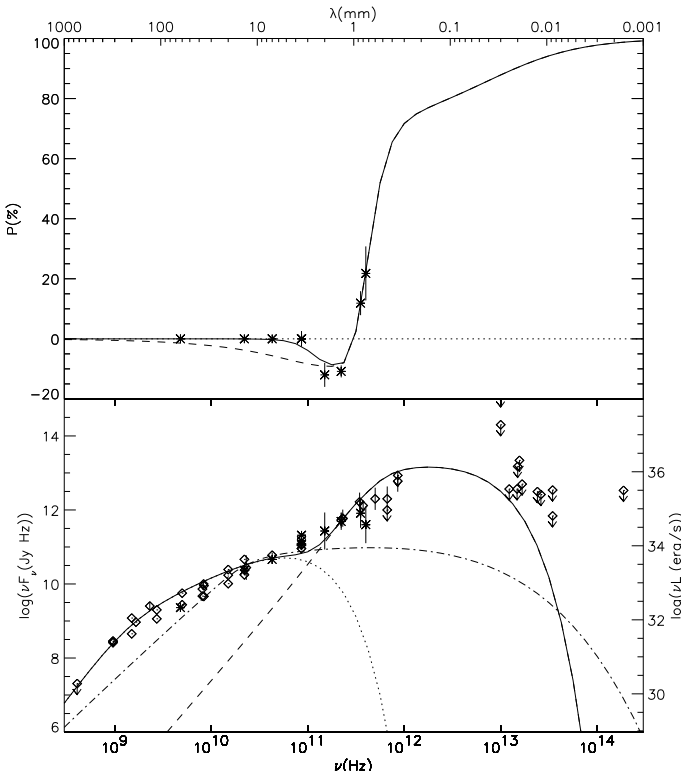


Fig. 1: Polarization and spectral energy distribution of Sgr A\* compared to model. The dashed line shows the polarized component, the dotted line the unpolarized, monoenergetic component, and the solid line the sum of the two. The dot-dash line shows the maximum CDAF model (assumed to be unpolarized; the total polarization is similar if the CDAF replaces the monoenergetic component). The diamonds are the data compiled by Narayan et al. (1995), while the asterisks are the data from Bower et al. (1999a,b) and A00.

Figure 1 compare the model to the data. To compare the polarization, we have plotted the Stokes' parameter that lies at  $83^\circ$ . Remarkably, the polarization should rise to  $\sim 100\%$  at even shorter wavelengths.

#### 4.1. Physical conditions in Synchrotron emitting regions

The brightness temperature of the polarized emission region is somewhat uncertain due to the unknown source size. Krichbaum et al. (1998) report a source radius of  $55\mu\text{as}$  at  $1.4$  mm from VLBI observations; this corresponds to  $19r_g$ . We expect the radius of the emission region to be greater than the size of the event horizon of the black hole, which has an apparent size of  $\sim 5r_g \sim 15\mu\text{as}$  projected on the sky (including gravitational bending, Bardeen 1973), so we use an intermediate size in further estimates. The flux of the fitted model at the self-

absorption frequency,  $\nu_t = 550$  GHz, is  $\sim 9$  Jy. This implies a brightness temperature in the emission frame  $T_b \sim 1.6 \times 10^{10}(r_s/10r_g)^{-2}\Gamma^{-1}$  K, where  $r_s$  is the size of the source (we have assumed the area of the source is  $\pi r_s^2$ ). For a steeply falling electron number distribution,  $kT_b \sim 4\gamma m_e c^2$  (for  $\xi = 2$ ), where  $\gamma m_e c^2$  is the energy of the emitting electrons, implying  $\gamma \sim 10(r_s/10r_g)^{-2}\Gamma^{-1}$  for the electrons at the self-absorption frequency. Using the formulae from §2, we find:  $B_\perp = 350(r_s/10r_g)^4\Gamma G$ ,  $\tau_C = 10^{-5}(r_s/10r_g)^{-8}\Gamma^{-5}$ , and  $\gamma_{max} = 50(r_s/10r_g)^{-2}\Gamma^{-1}$ , implying  $n_e \sim 6 \times 10^6(r_s/10r_g)^{-9}\Gamma^{-5}\text{cm}^{-3}$ . The ratio of magnetic to rest-mass energy density is  $B^2/(8\pi n_e m_p c^2) \sim 1(r_s/10r_g)^{17}\Gamma^{9/2}$  for an electron-proton plasma, indicating a relativistic Alfvén speed. The Faraday rotation angle at  $\nu_t = 5.5 \times 10^{11}$  Hz is  $\Delta\theta \sim 350(r_s/10r_g)^{-4}\Gamma^{-2}\gamma_{min}^{-3}$ , assuming  $B_\parallel \sim B_\perp$ . For  $r_s \sim 10r_g$ ,  $\gamma_{min}$  can be as large as  $4$ , reducing  $\Delta\theta$  to  $5$ ; for  $r_s \sim 5r_g$ ,  $\gamma_{min}$  can be as large as  $20$  reducing  $\Delta\theta$  to  $\sim 0.6$ . Alternatively, if the synchrotron emission is due to a pair plasma, Faraday rotation will be reduced by the ratio of the proton number density to the pair number density. The rotation angle is further reduced at the observed wavelengths by a factor  $\sim \nu/\nu_t$ . The high energy cutoff for the electron distribution may be due to synchrotron cooling since  $t_{cool} = 8 \times 10^8\gamma_{max}^{-1}B^{-2} \sim 6(r_s/10r_g)^{-6}\Gamma^{-3}$  sec, similar to the dynamical time,  $t_D \sim 13x^{-3/2}$  sec.

The unpolarized emission component dominates at  $\sim 7$  mm, where Lo et al. (1998) measure a source size of  $\sim 5 \times 10^{13}$  cm. The self-absorption frequency then requires  $\gamma \sim 400$ ,  $B \sim 0.1$  G, and  $n_e \sim 4 \times 10^5 \text{ cm}^{-3}$ . Though somewhat ad-hoc, this model reproduces the spectrum well. The Faraday rotation parameter is rather small, so depolarization requires field which is tangled on a scale  $\sim 100$  times smaller than the size of the emission region.

#### 4.2. Accretion Component

We have tried modeling the spectrum of the unpolarized component with a self-similar, self-absorbed accretion flow. We used the cyclo-synchrotron emission formulae from Mahadevan, Narayan, & Yi (1996) and we performed the radiation transfer in full general relativity (Kurpiewski & Jaroszyński 1997). We can place an upper limit on the accretion rate of an ADAF component (using the model of Özel et al. 2000) since its unpolarized flux must not dilute the polarized component: we find  $\dot{M}_{ADAF} \lesssim 3 \times 10^{-6} M_\odot/\text{yr}$ . If the ADAF surrounds the polarized emission region, then it will depolarize, so the Faraday depolarization places a stronger upper limit (§2). We can place a similar limit on the CDAF model (using the structure from Quataert & Gruzinov, 2000, with equipartition  $B$  field and  $p_{gas} = 2n_e k_B T_e$ ): we find  $\dot{M}_{CDAF} \lesssim 1.5 \times 10^{-9} M_\odot/\text{yr}$ ; this accretion rate can account for the unpolarized component at  $\nu \gtrsim 10$  GHz (see Figure 1) and is consistent with the Faraday rotation constraint. The CDAF luminosity is  $2 \times 10^{34} \text{ erg/s}$  and the self-absorption frequency is  $\sim 30$  GHz, so the polarized component would be visible through it. Finally, we can place a limit on a standard thin disk from the infrared upper limits: we find  $\dot{M}_{thin} \lesssim 2 \times 10^{-11} M_\odot/\text{yr}$ ; this upper limit can be increased to a maximum of  $3 \times 10^{-7} M_\odot/\text{yr}$  if the inner edge of the disk is truncated at  $r = 6000r_g$ .

## 5. CONCLUSIONS

The main success of advection-dominated accretion models for Sgr A\* is in explaining the high-frequency radio spectrum and skirting below the upper limits at infrared frequencies. However, the ADAF model is unpolarized at the same high frequencies, inconsistent with the recent detection of linear polarization. We have constructed a simple toy model for the millimeter polarization which predicts a rise towards shorter wavelengths: polarization of  $\sim 70\%$  might be seen with SCUBA at  $350\text{ }\mu\text{m}$  if this model is correct. The lack of polarization and spectral slope of  $1/3$  at wavelengths longer than  $2\text{ mm}$  indicates that a different physical component may be contributing. The presence of two physical components can be confirmed by looking for a change in variability amplitude and time-scale or source size and morphology around  $2\text{ mm}$ .

The high observed polarization implies a highly ordered magnetic field lying near the sky plane. This might be due to the poloidal field in a jet seen edge-on. The non-thermal electron distribution might be produced by shock acceleration, reconnection, or electric field acceleration near the event horizon of a spinning black hole (Blandford & Znajek 1977). The Blandford-Znajek mechanism can generate a maximum luminosity of  $L_{BZ} \sim 10^{37}(B/600\text{G})^2\text{ erg/s}$  (Thorne, Price, & MacDonald 1986), so the entire polarized luminosity of Sgr A\* might be powered by black hole spin.

The dynamics of the emission region will be controlled by the ratio of the magnetic field energy density to the matter energy density,  $B^2/(8\pi\rho c^2)$ ; however, this ratio scales as  $r_s^{17}\Gamma^{9/2}$ , while  $\Gamma$  and  $r_s$  are unknown. Doppler boosting decreases the brightness temperature, which reduces Faraday rotation but makes the electrons trans-relativistic. Future sub-mm VLBI observations should accurately measure the  $r_s$  as a function of frequency, and proper motions may constrain  $\Gamma$ . Also uncertain are the pair fraction and minimum electron energy  $\gamma_{min}$ . The pair number density can be constrained by measuring the circular polarization; without pairs, the circular polarization may be as high as a few percent at optically-thin wavelengths (Jones & O'Dell 1977), while pure pair emission should have no circular polarization. The pair annihilation line should be looked for at higher spatial resolution; however, it will be strongly broadened by relativistic mo-

tions of the pairs. Once the source size is known,  $\gamma_{min}$  and the pair fraction will be constrained by the Faraday rotation limit.

An ADAF model must have a low accretion rate,  $\lesssim 10^{-8}M_\odot/\text{yr}$ , to be consistent with the lack of Faraday rotation of the polarized emission. Such a low inferred accretion rate disagrees with estimates of the Bondi accretion rate inferred from stellar winds near the region of the black hole. If accretion is episodic due to outer-disk instabilities, then the current state might be one of low accretion rate in the inner disk. Alternatively, the accretion rate might be reduced by depositing energy from the accretion flow in the surrounding gas (either through outflow or convection), thus increasing the sound speed and decreasing the capture rate of gas by the black hole. The accretion flow must deposit energy  $\dot{M}_A GM/r_A \sim 6 \times 10^{35}\text{ erg/s}$ , where  $\dot{M}_A$  is the stellar mass loss rate which crosses the Bondi radius  $r_A$  (Quataert et al. 1999). This can be supplied by accretion which releases energy  $\sim 5 \times 10^{35}(\eta/0.01)\dot{m}_{-9}\text{ erg/s}$ , where  $\eta$  is the efficiency with which accretion deposits energy at large radius. As remarked above, a convection-dominated accretion flow with  $\dot{M} \sim 10^{-9}M_\odot/\text{yr}$  can explain part of the unpolarized component without diluting the polarized emission; the associated convection can carry the required energy outward to suppress the Bondi accretion rate.

Since the self-absorption frequency occurs at  $\sim 500\mu\text{m}$ , it will be possible to image shadow of a black hole from the ground using VLBI, providing a direct confirmation of the existence of an event horizon (Falcke, Melia, & Agol 2000). Future sub-mm polarimetric VLBI observations might show rotation of the polarization angle near the black hole, a general relativistic effect which becomes stronger for a spinning black hole (Connors, Stark, & Piran 1980).

Eliot Quataert & Andrei Gruzinov have shown me work which reaches similar conclusions about ADAFs, but attributes the polarization swing to magnetic field geometry rather than self-absorption.

I acknowledge Ski Antonucci, Julian Krolik, Colin Norman, and Eliot Quataert for ideas and corrections which greatly improved this letter. This work was supported by NSF grant AST 96-16922.

## REFERENCES

Agol, E. & Blaes, O. M., 1996, MNRAS, 292, 965  
 Aitken, D. K., et al., 2000, ApJ, in press, astro-ph/0003379, A00  
 Bardeen, J. M. 1973, in Black Holes, ed. C. DeWitt & B. S. DeWitt (New York: Gordon & Breach), 215  
 Begelman, M. C. & Blandford, R. D., 1999, MNRAS, 303, L1  
 Bower, G. C., Backer, D. C., Zhao, J. H., Goss, M., & Falcke, H. 1999a, ApJ, 521, 582  
 Bower, G. C., Wright, M. C. H., Backer, D. C., & Falcke, H. 1999b, ApJ, 527, 851  
 Beckert, T. & Duschl, W. J., 1997, A & A, 328, 95  
 Blandford, R. D. & Znajek, R. L. 1977, MNRAS, 179, 433  
 Coker, R. & Melia, F., 1999, ApJ, 511, 750  
 Connors, P. A., Stark, R. F., & Piran, T., 1980, ApJ, 235, 224  
 Falcke, H., Mannheim, K., & Biermann, P. L., 1993, A&A, 278, L1  
 Falcke, H., Melia, F., & Agol, E., 2000, ApJ, 528, L13  
 Genzel, R., Eckart, A., Ott, T., & Eisenhauer, F., 1997, MNRAS, 291, 219  
 Ghez, A. M., Klein, B. L., Morris, M., & Becklin, E. E. 1998, ApJ, 509, 678  
 Ginzburg, V. L. & Syrovatskii, S. I., 1965, ARA&A, 3, 297, GS  
 Ginzburg, V. L. & Syrovatskii, S. I., 1969, ARA&A, 7, 375, GS  
 Krichbaum, T. P. et al. 1998, A&A, 335, L106  
 Lo, K. Y., Shen, Z. Q., Zhao, J. H., & Ho, P. T. P. 1998, ApJ, 508, L61  
 Kurpiewski, A. & Jaroszyński, M., 1999, A&A, 346, 713  
 Jones, T. W. & Hardee, P. E., 1979, ApJ, 228, 268  
 Jones, T. W. & O'Dell, S. L., 1977, ApJ, 214, 522  
 Mahadevan, R., 1999, MNRAS, 304, 501  
 Mahadevan, R., Narayan, R., & Yi, I., 1996, ApJ, 465, 327  
 Melia, F., 1992, ApJ, 387, L25  
 Narayan, R. & Yi, I., 1994, ApJ, 428, L13  
 Narayan, R., Yi, I., & Mahadevan, R., 1995, Nature, 374, 623  
 Özel, F., Psaltis, D., & Narayan, R., 2000, ApJ, in press, astro-ph/0004195  
 Quataert, E., Narayan, R., & Reid, M. J., 1999, ApJ, 517, L101  
 Quataert, E. & Narayan, R., 1999, ApJ, 520, 298  
 Quataert, E. & Gruzinov, A., 2000, ApJ, in press, astro-ph/9912440  
 Stone J. M., Pringle J. E., & Begelman M. C., 1999 MNRAS, 310, 100  
 Thorne, K. S., Price, R. H., & Macdonald, D., 1986, Black Holes: The Membrane Paradigm. Yale Univ. Press, New Haven, CN